Temperature dependent structural evolution in liquid $Ag_{50}Ga_{50}$ alloy

Y Su[1], X D Wang[1,*], Q Yu[1], Q P Cao[1], U Ruett[2], D X Zhang[3] and J Z Jiang[1,*]

[1]*International Center for New-Structured Materials (ICNSM), Laboratory of New-Structured Materials, State Key Laboratory of Silicon Materials, and School of Materials Science and Engineering, Zhejiang University, Hangzhou, 310027, People's Republic of China*

[2]*Deutsches Elektronen Synchrotron (DESY), Notkestraße 85, 22607 Hamburg, Germany*

[3]*State Key Laboratory of Modern Optical Instrumentation, Zhejiang University, Hangzhou, 310027, People's Republic of China*

*Corresponding author: wangxd@zju.edu.cn and jiangjz@zju.edu.cn

Abstract

The temperature dependence of atomic structural evolution in the liquid $Ag_{50}Ga_{50}$ alloy has been studied by using *in situ* high energy X-ray diffraction (XRD) experiment combined with the first-principles molecular dynamics (FPMD) simulations. The experimental data show a reversible structural crossover at the temperature about 1050 K. Changes in both electrical resistivity and absolute thermoelectric power at about 1100 K strongly support the XRD results. Additionally, FPMD simulations reveal an abnormal temperature dependent behavior of partial coordination number and atomic diffusivity at about 1200 K, elucidating that the partition experimentally observed changes in structure and properties could be linked with the repartition between Ag and Ga atoms in the liquid at around 1050-1200 K. This finding will trigger more studies on the structural evolution of noble-polyvalent metals in particular and metallic liquids in general.

Keywords: Liquid $Ag_{50}Ga_{50}$ alloy, Structural evolution, Noble-polyvalent metallic liquids

1. Introduction

Amorphous alloys (AAs) have been received considerable attention due to their excellent mechanical, magnetic, corrosion and superelastic deformation properties, but their atomic structure is still perplexed as compared to their crystalline counterparts. AAs can be fabricated by rapidly quenching from melts by copper mold. This is the reason that AAs are sometimes termed as frozen melts. Hence, tracking the structural evolution in melts changing with temperatures can not only deepen the understanding of the glass formation, but also uncover novel phenomena in the liquid state. For example, metallic liquids of noble metals with polyvalent elements often show non-linear magnetic, electric and/or thermodynamic properties [1-11]. Vinckel et al. [11] found non-linear changes in the electrical resistivity and absolute thermoelectric power in liquid silver-gallium (Ag-Ga) alloys with different compositions, which is a prototype model system for studying noble-polyvalent metallic alloys, such as Ag-Ge, Ag-In, Cu-Ga, Au-Ga. Shirakawa et al. [12] proposed the correlation of electronic density of states with the concentration-concentration fluctuation in the long-wavelength limit in liquid Ag-polyvalent alloys, and further pointed out that liquid noble-polyvalent metals could have short range ordered states when the atomic size ratio for the constituents is less than 1.4. Kaban et al. [13] assumed the existence of electronically stabilized clusters of pure elements (either noble or polyvalent metal depending on the concentration of the alloy) in the liquid noble-polyvalent alloys, which was caused by topological and chemical short-range ordering in the liquid state. However, due to the lacking of solid evidences from advanced experimental techniques, e.g., *in situ* high energy X-ray diffraction (XRD), and analytical methods, e.g., first-principles molecular dynamics (FPMD) simulations, whether the anomalous structural evolution, e.g., the liquid-to-liquid transition, exists in noble-polyvalent metallic systems is still uncertain. Here, we report results of temperature dependent structural data for a liquid $Ag_{50}Ga_{50}$ alloy obtained by *in situ* high energy XRD and FPMD simulations in a temperature range of 790 K -1260 K. We reveal a reversible structural crossover at about 1050 K, resulting in a kink in atomic diffusivity, partial coordination number (CN), electrical resistivity and absolute thermoelectric power and a deviation from linear temperature dependence of first and second peak positions in structure factor *S(q)* and reduced pair distribution function *G(r)*. This

finding will trigger more studies on the structural evolution in noble-polyvalent metallic liquids.

2. Methods

Using purity Ag (99.999%) and Ga (99.999%) slugs, $Ag_{50}Ga_{50}$ alloy was prepared by arc melting. To ensure the chemical homogeneity, the ingots were remelted more than five times. The sample was sealed in quartz capillaries with 1.5 mm diameter under a vacuum of about 4.6×10^{-3} Pa. *In situ* high temperature and high energy synchrotron XRD measurements were carried out at the beamline P07 at PETRA III, Deutsches Elektronen Synchrotron (DESY), Hamburg with the beam size of about 0.8×0.8 mm^2 and wavelength of 0.1256 Å. The sealed tube was heated in a three-lamp-focused furnace with the same heating and cooling rates of 12 K/min. A flat panel Si detector (Perkin Elmer 1621, 200×200 μm^2 pixel size, 2048×2048 pixels) was applied to collect experimental data with an exposure time of 5 s. Two thermocouples were used to measure the temperature change, which was calibrated by temperature dependent lattice parameter of crystalline silicon. The effective temperature range to measure the $Ag_{50}Ga_{50}$ liquid was from 790 K to 1260 K. The pattern from an empty capillary with the same diameter and exposure time was used as a background. Scattering intensity *I(q)* was integrated by 2D diffraction patterns under the software package FIT2D [14]. The total structure factor *S(q)* was obtained from *I(q)* after subtracting the appropriate background by using software package PDFgetX3 [15], which is based on the Faber-Ziman formalism [16],

$$S(q) = 1 + \frac{I(q) - [\sum_{i=1}^{N} c_i f_i^2(q)]}{[\sum_{i=1}^{N} c_i f_i(q)]^2} \quad (1)$$

where $f_i(q)$ is the X-ray scattering factor of the atom i and c_i is the atomic concentration of species i (i=Ag, Ga). Subsequently, the reduced pair distribution function *G(r)* was obtained by a sine Fourier transformation of the total structure factor *S(q)*.

$$G(r) = 4\pi r[\rho(r) - \rho_0] = \frac{2}{\pi}\int_0^{\infty} q[S(q) - 1]\sin(rq)dq \quad (2)$$

The first-principle molecular dynamics (FPMD) simulations of liquid $Ag_{50}Ga_{50}$ alloy were performed by the density functional theory (DFT) with the Vienna *ab initio* simulation package (VASP) [17,18]. The projector augmented wave (PAW) method [19] with the generalized

gradient approximation (GGA) in the form by Perdew-Burke-Ernzerhof (PBE) [20] was applied to describe the interaction between electrons and ions. The canonical NVT ensemble (constant atom number, volume and temperature) was used in the FPMD simulations [21-24] and the Nosé-Hoover thermostat was applied to control the system temperature [25,26]. The Newton's equations of motion were integrated with the velocity Verlet algorithm and a time step of 3 fs [26]. In FPMD simulations, a cubic cell containing 200 atoms (100 Ag atoms and 100 Ga atoms) is built with periodic boundary conditions. In order to remove the memory effect of the initial configuration, the cell was heated up to 2000 K and relaxed for 6000 steps, then quenched to 1500, 1400, 1300, 1200, 1100, 1000, 900, 800 and 700 K with a cooling rate of 3.33×10^{13} K/s. At each temperature, the size of cell was adjusted to make sure that the average internal pressure was close to zero within ±0.5 kbar. Then another 6000 steps were carried out for structural relaxation and only last 3000 steps were selected for structure analyses.

3. Results and discussion

High quality total structure factor data *S(q)* during both heating and cooling procedures in a temperature range from 790 K to 1260 K for liquid $Ag_{50}Ga_{50}$ alloy were recorded in Figs. 1(a) and (b), respectively, while Figs. 1(c) and (d) show the temperature dependent reduced pair distribution function *G(r)* in a temperature range of 790 K to 1260 K for liquid $Ag_{50}Ga_{50}$ alloy obtained by Fourier transformation of *S(q)* during heating and cooling procedures, respectively. Peak positions of the first and second peaks in *S(q)* and *G(r)* curves and their ratios during heating and cooling processes are plotted in Figs. 2(a-f), respectively. Considering the symmetrical peak profiles, we applied a Gauss function plus a linear baseline to fit the peaks of *G(r)* curves and the second peak of *S(q)* curves and achieved good fittings. Due to the relatively sharp profile of first peak of *S(q)*, we found that using Lorentz function is much better than Gauss function to fit the profile. The results show that peak positions of the first and second peaks of *S(q)* and *G(r)* curves coincide well during heating and cooling procedures, indicating a reversible structural evolution happens in the liquid $Ag_{50}Ga_{50}$ alloy. The peak positions of the first peak in both *S(q)* and *G(r)* shift to low values as the temperature increases from 790 K to 1260 K, indicating that the whole liquid $Ag_{50}Ga_{50}$ alloy expands while the

nearest neighbor distance between the center atom and atoms at the first shell shrinks when the temperature increases. The 'contradiction behavior' for the first peak positions of *S(q)* and *G(r)* are due to different correlation lengths. One generally considers that the first peak position of *S(q)* is linked with liquid density, i.e., the lower the peak position, the lower the density. Because of the expansion of the whole liquid during heating, the density of the liquid decreases with temperature, leading to the decrease of the first peak position of *S(q)*. However, the first peak of *G(r)* deduced by XRD reveals only the atomic packing (relative high scattering of X-ray in denser atomic clusters) in short range (most likely less than 5 Å). It should be stressed that X-ray scattering power from the free volume part induced by temperature between clusters in liquid are much weaker as compared to denser atomic clusters. In our previous work [27], we clearly revealed the negative expansion on the short-range local atomic scale in *G(r)* in metallic liquids during heating while whole liquids all expand during heating. On the other hand, peak positions of the second peak in both *S(q)* and *G(r)* shift to high values as the temperature increases from 790 K to 1260 K, indicating abnormal behavior in the interior local atomic structure in the liquid $Ag_{50}Ga_{50}$ alloy, e.g., the formation of more free volume between different atomic clusters during heating. By guiding of the linear lines in Figs. 2(a-f), it is noteworthy that the peak positions of the first and second peaks in both *S(q)* and *G(r)* and their ratios deviate from the linear feature at almost the same temperature of about 1050 K. This fact might suggest the existence of some kinds of structural changes in short and/or medium ranges below and above about 1050 K, but more evidence are strongly desirable to support the structural crossover in the liquid $Ag_{50}Ga_{50}$ alloy.

In order to elucidate the results obtained from *in situ* high energy XRD experiments and to understand the local atomic packing and structural evolution in the liquid $Ag_{50}Ga_{50}$ alloy, first-principle molecular dynamics (FPMD) simulations were conducted. The simulated total structure factor *S(q)* and pair correlation function *g(r)* at various temperatures are plotted in Figs. 3(a) and (b) together with the experimental data, respectively. It is clear that the calculated *S(q)* and *g(r)* data match well with the experimental *S(q)* and *g(r)* data at corresponding temperatures, indicating that FPMD could provide us with reliable atomic configurations for structural analyses. As shown in Figs. 3 (c) and (d), the total and partial coordination numbers

(CN) for the nearest neighbor atoms were calculated by using the Voronoi tessellation method [28] which divides the three-dimensional space into various polyhedral cells (or called Voronoi polyhedron (VP)) constructed by a center atom and its nearest-neighboring atoms, offering a method to analyze the local atomic packing. The cutoff value between the center atom and its neighbor atoms was estimated at the minimum position of the right side of the first peak of simulation *g(r)* data. The total number of polygons of the VP is equivalent to the coordination number (CN) for a selected central atom. For the experimental nearest-neighboring CN, we integrated the first peak of radial distribution functions (RDF) derived from *G(r)* data using the following equation

$$RDF = 4\pi r^2 \rho_0 + rG(r) \tag{3}$$

where ρ_0 is the number density at various temperatures. Note that it is very hard to experimentally obtain the partial *g(r)* and partial CN, however, FPMD simulations can easily estimate partial *g(r)* and partial CN, e.g., $CN_{Ag\text{-}Ga}$, $CN_{Ga\text{-}Ag}$, $CN_{Ag\text{-}Ag}$ and $CN_{Ga\text{-}Ga}$ from the atomic configurations at various temperatures. It is found in Fig. 3(c) that the total CN deduced from both experiments and simulations increases with decreasing temperature. By a carefully check, it seems that at about 1050 K-1200 K, the slopes of the temperature dependent CN change, which become more clearly on the temperature dependent partial CNs in Fig. 3(d). At 1200 K -1300 K, kinks are detected for $CN_{Ag\text{-}Ga}$, $CN_{Ga\text{-}Ag}$, $CN_{Ag\text{-}Ag}$ and $CN_{Ga\text{-}Ga}$. At 1200 K, the $CN_{Ag\text{-}Ag}$ has an abrupt increment from 5.48 to 5.67, the $CN_{Ga\text{-}Ga}$ raises from 5.27 to 5.43, while both $CN_{Ag\text{-}Ga}$ or $CN_{Ga\text{-}Ag}$ show sudden declines from 6.08 to 5.84. These results suggest a repulsive interaction between Ag and Ga atoms, i.e., Ag atoms prefer to gather with Ag atoms while Ga atoms prefer to gather with Ga atoms at around 1200 K upon heating. These obtained results in Fig. 3 are consistent with the temperature dependent peak position data of the first and second peaks in *S(q)* and *G(r)* curves in Fig. 2. The slight difference in temperature between experiments and simulations could be caused by the different cooling rates used, which are 0.2 K/s in experiment and 3.33×10^{13} K/s in simulation.

The above results suggest that a structural crossover at around 1050-1200 K occurs in the liquid $Ag_{50}Ga_{50}$ alloy. If it is true, most likely, properties (e.g., diffusivity, thermoelectric power and electrical resistivity) of liquid $Ag_{50}Ga_{50}$ alloy should be affected. Fig. 4(a) shows the self-

diffusion coefficients (*D)* of liquid $Ag_{50}Ga_{50}$ alloy at various temperatures, which are derived from the mean square displacement with the Stokes-Einstein equation

$$D = \lim_{t\to\infty} \frac{\left\langle \left| R_i(t) - R_i(0) \right|^2 \right\rangle}{6t} \tag{4}$$

where $R_i(t)$ is the atomic position of atom *i* at time *t* and $R_i(0)$ is the atomic position of atom *i* at the initial time. It should be stressed that a linear mean square displacement as the function of time were reached at each temperature. In Fig. 4(a), the error bars of self-diffusion coefficients (*D*) of total, Ag and Ga atoms are drawn about 1×10^{-6} cm^2/s which are small and similar to the symbol sizes. Within the error bars, one can clearly reveal that no matter for total, Ag or Ga atoms, a kink at about 1200 K is clearly observed. The activation energy of about 14.8 kJ/mol for Ag atoms and 13.5 kJ/mol for Ga atoms at the low-temperature range (below ~1200 K) changes to 21.1 kJ/mol for Ag atoms and 20.7 kJ/mol for Ga atoms at high-temperature region (above ~1200 K), respectively. It is clear that the activation energies for diffusion of Ag and Ga in the range of above ~1200 K are found to be higher than those in the range of below ~1200 K. This phenomenon is in contrast to the common sense that for a uniform liquid system, the activation energy at high temperatures should be lower than that at low temperatures. It also indicates the existence of a structural crossover in the liquid $Ag_{50}Ga_{50}$ alloy at around 1200 K. In addition, Fig. 4(b) is the reported data of the temperature dependent electrical resistivity and thermoelectric power data for the liquid $Ag_{50}Ga_{50}$ alloy [11]. Changes in both electrical resistivity and thermoelectric power curves at around 1100 K can be clearly observed. This data corroborate our results well, strongly suggesting that the liquid $Ag_{50}Ga_{50}$ alloy does exhibit a liquid-to-liquid crossover at about 1050 K in terms of changes in structure and properties.

4. Conclusions

The structural evolution of liquid $Ag_{50}Ga_{50}$ alloy has been studied by *in situ* high-energy XRD measurements and FPMD simulations. Experimental results, i.e., temperature dependent peak positions of the first and second peaks in *S(q)* and *G(r)* curves, the nearest neighbor coordination number (CN), the reported electrical resistivity and the absolute thermoelectric power, uncovered an intriguing structural change in the liquid $Ag_{50}Ga_{50}$ alloy at temperature

of about 1050 K. Such structural changes at about 1050 K in the liquid $Ag_{50}Ga_{50}$ alloy are reversible during heating and cooling procedures. FPMD simulations reproduce the experimental observations. At about 1050 K -1200 K, the slopes of the temperature dependent total CN change lightly and the partial CNs of Ag-Ag and Ga-Ga increase while the partial CNs of Ag-Ga and Ga-Ag decrease, indicating that the rearrangement of Ag and Ga atoms in liquid at about 1050 K -1200 K causes the experimentally observed structural changes in the liquid $Ag_{50}Ga_{50}$ alloy. Meanwhile, an abnormal temperature dependent behavior of atomic diffusivity at about 1200 K further supports this conclusion, i.e., liquid $Ag_{50}Ga_{50}$ alloy does have a liquid-to-liquid crossover at about 1050 K in terms of changes in structure and properties. The slight difference in temperature between experiments and simulations could be caused by the different cooling rates used. It is no doubt that our discovery could promote the understanding of the structural evolution in noble-polyvalent metallic melts in particular and metallic liquids in general.

Acknowledgements

Financial supports from the National Key Research and Development Program of China (No. 2016YFB0701203 and 2016YFB0700201), the National Natural Science Foundation of China (U1432110, U1532115, 51671170 and 51671169), the Natural Science Foundation of Zhejiang Province (grants Z1110196 and Y4110192), and the Fundamental Research Funds for the Central Universities are gratefully acknowledged. The computer resources at National Supercomputer Centers in Tianjin and Guangzhou are also gratefully acknowledged. Synchrotron radiation experiments were carried out at the light source PETRAIII at DESY, a member of the Helmholtz Association (HGF).

References:

[1] Terzieff P 2003 *Phys. Chem. Liquids* **41** 431

[2] Arai Y, Shirakawa Y, Tamaki S, Azuma M 1995 *J. Phys. Soc. Jpn.* **64** 2594

[3] Qi G J, Hino M, Azakami T 1989 *Mater. Trans.* **30** 575

[4] Xiong L H, Chen K, Ke F S, Lou H B, Yue G Q, Shen B, Dong F, Wang S Y, Chen L Y, Wang C Z, Ho K M, Wang X D, Lai L H, Xie H L, Xiao T Q, Jiang J Z 2015 *Acta Mater.* **92** 109

[5] Terzieff P, Tsuchiya Y 2001 *J. Phys.: Condens. Matter* **13** 3573

[6] Jendrzejczyk D, Fitzner K 2005 *Thermochim. Acta* **433** 66

[7] Terzieff P, Komarek K L, Wachtel E 1986 *J. Phys. F: Met. Phys.* **16** 1071

[8] Jena A K, Ramachandran T R 1971 *Metall. Mater. Trans. B* **2** 2958

[9] Wasai K, Kano M, Mukai K 1995 *Int. J. Thermophys.* **16** 831

[10] Venkatesh R, Mishra R K 2005 *J. Non-Cryst. Solids* **351** 705

[11] Vinckel J, Hugel J, Gasser J G 1996 *Philos. Mag. B* **73** 231

[12] Shirakawa Y, Arai Y, Iida T, Tamaki S 1998 *Thermochim. Acta* **314** 291

[13] Kaban I, Hoyer W 2002 *J. Non-Cryst. Solids* **312** 41

[14] Hammersley A P, Svensson S O, Hanfland M, Fitch A N, Hausermann D 1996 *High Pressure Res.* **14** 235

[15] Juhás P, Davis T, Farrow C L, Billinge S J L 2012 *J. Appl. Crystallogr.* **46** 560

[16] Faber T E, Zimman J M 1965 *Phil.Mag.* **11** 153

[17] Kresse G, Furthmüller J 1996 *Comp. Mater. Sci.* **6** 15

[18] Kresse G, Furthmüller J 1996 *Phys. Rev. B* **54** 11169

[19] Blöchl P E 1994 *Phys. Rev. B* **50** 17953

[20] Perdew J P, Burke K, Ernzerhof M 1996 *Phys. Rev. Lett.* **77** 3865

[21] Kresse G, Hafner J 1993 *Phys. Rev. B.: Condens. Matter* **47** 558

[22] Zhang D X, Shen B, Zheng Y X, Wang S Y, Zhang J B, Yang S D, Zhang R J, Chen L Y, Wang C Z, Ho K M 2014 *Appl. Phys. Lett* **104** 121907

[23] Zhu M, Xia M J, Rao F, Li X B, Wu L C, Ji X L, Lv S L, Song Z T, Feng S L, Sun H B, Zhang S B 2014 *Nat. Commun.* **5** 4086

[24] Zhang H, Shang S L, Wang W Y, Wang Y, Hui X D, Chen L Q, Liu Z K 2014 *Comput. Mater. Sci.* **89** 242

[25] Nosé S 1984 *J. Chem. Phys.* **81** 511

[26] Hoover W G 1985 *Phys. Rev. A* **31** 1695

[27] Lou H B, Wang X D, Cao Q P, Zhang D X, Zhang J, Huc T D, Maoa H K, Jiang J Z 2013 *PNAS*

110 10068

[28] Finney J L, *Nature* **266** 309

Figure captions

Fig. 1 (a) and (b) Waterfall graphs of temperature dependent experimental total structure factors $S(q)$ of liquid $Ag_{50}Ga_{50}$ alloy obtained from *in situ* high temperature high energy synchrotron XRD measurements for the heating and cooling procedures in the temperature range of 790 K -1260 K, respectively. (c) and (d) Waterfall graphs of temperature dependent experimental reduced pair distribution functions *G(r)* of liquid $Ag_{50}Ga_{50}$ alloy obtained from Fourier transformation of *S(q)* during heating and cooling procedures in the temperature range of 790 K -1260 K, respectively.

Fig. 2 (a-c) Peak positions of the first and second peaks in *S(q)* curves and its ratio for liquid $Ag_{50}Ga_{50}$ alloy as a function of temperature, respectively. (d-f) Peak positions of the first and second peaks in *G(r)* curves and its ratio for liquid $Ag_{50}Ga_{50}$ alloy at various temperatures, respectively. Red open circles represent the heating procedure in the temperature range of 790 K -1260 K, while the blue open squares symbolize the cooling procedure. Guided by the black full lines and arrows, a deviation from linear evolution of the first and second peak positions in *S(q)* and *G(r)* curves and their ratios at about 1050 K is observed in the liquid $Ag_{50}Ga_{50}$ alloy.

Fig. 3 Comparisons of (a) total structure factors *S(q)* and (b) pair correlation functions *g(r)* by FPMD simulations and XRD experiments for the liquid $Ag_{50}Ga_{50}$ alloy, respectively. The black open circles represent the FPMD results and the color lines stand for the corresponding experimental data at various temperatures. Experimental g*(r)* is converted from *G(r)* data by $g(r) = 1 + \frac{G(r)}{4\pi\rho r}$, where ρ is the number density at various temperatures. (c) The total nearest neighbor coordination number (CN) at various temperatures of liquid $Ag_{50}Ga_{50}$ alloy. Blue open circles are the experimental data obtained from the first peak of radial distribution functions (RDF) and black solid spheres represent the total CNs obtained from the Voronoi polyhedra. The full lines illustrate the non-linear relationship of temperature dependent total nearest neighbor CN. (d) The partial CNs for Ag-centered and Ga-centered Voronoi polyhedra at various temperatures in the liquid $Ag_{50}Ga_{50}$ alloy. The yellow area labels the abnormal jump of the partial CNs.

Fig. 4 (a) Temperature dependent self-diffusion coefficients, *D*, for total atoms, Ag atoms and Ga atoms from 700 K to 1500 K in the liquid $Ag_{50}Ga_{50}$ alloy obtained from FPMD simulations. (b) The reported electrical resistivity and thermoelectric power of liquid $Ag_{50}Ga_{50}$ alloy as a function of temperature [11]. The lines are the guide for the eyes.

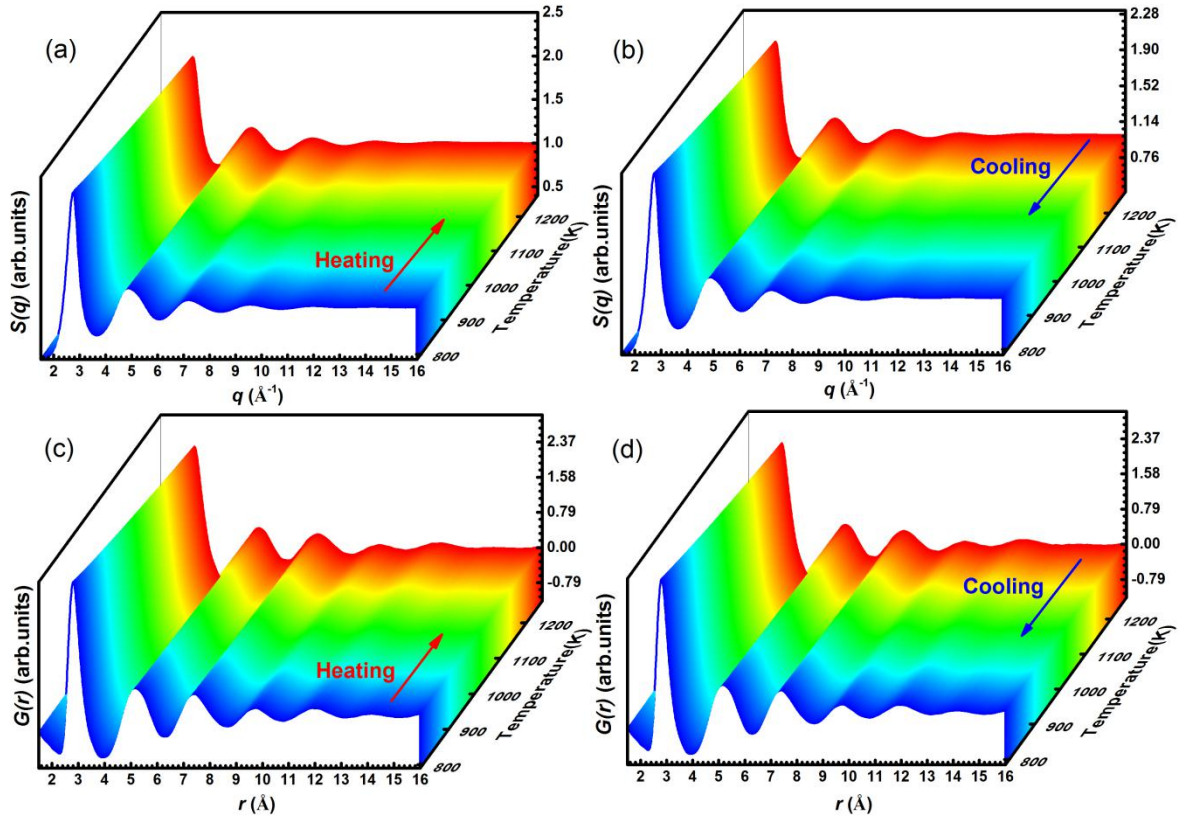

Fig. 1 Y. Su et al.,

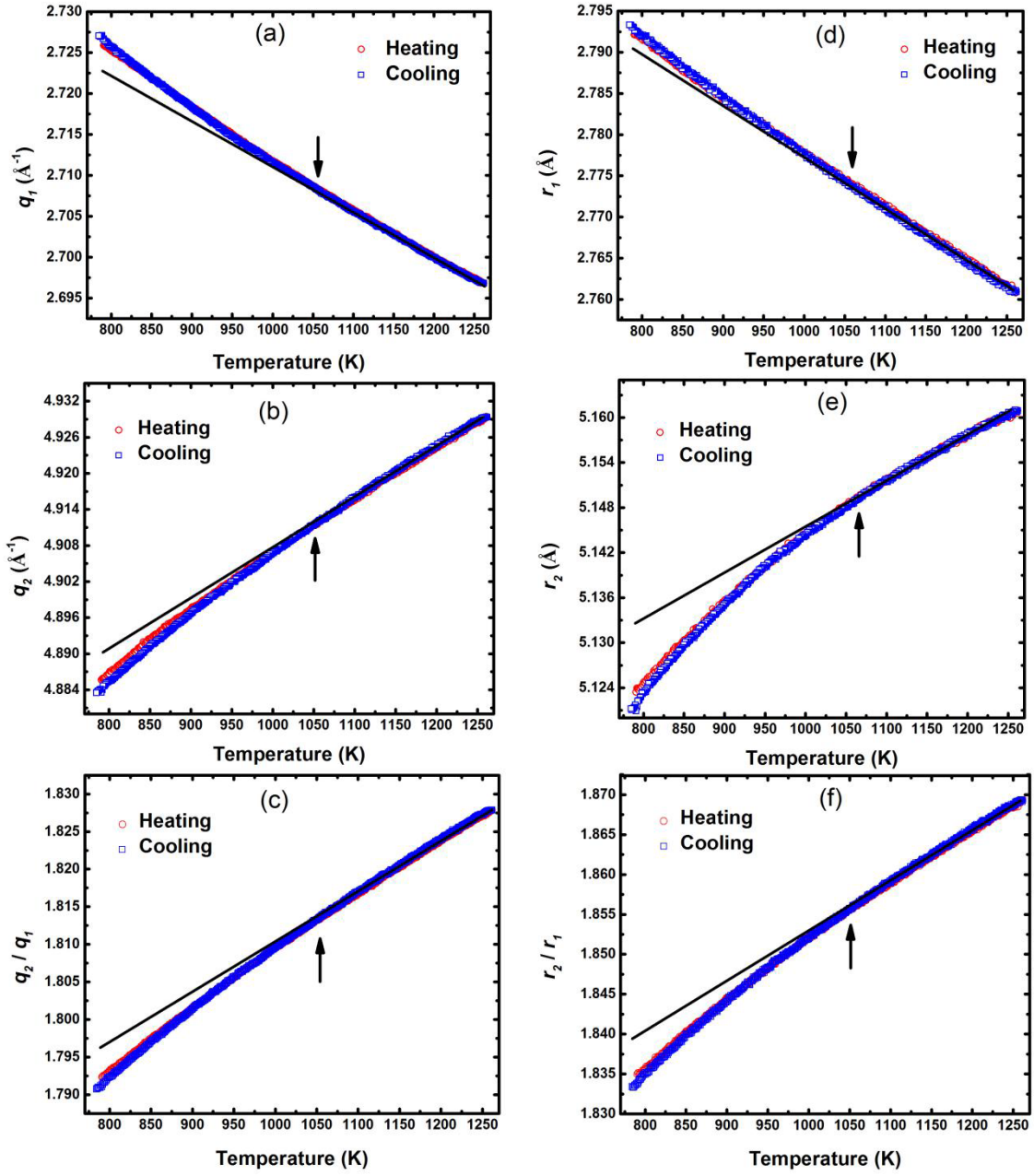

Fig. 2 Y. Su et al.,

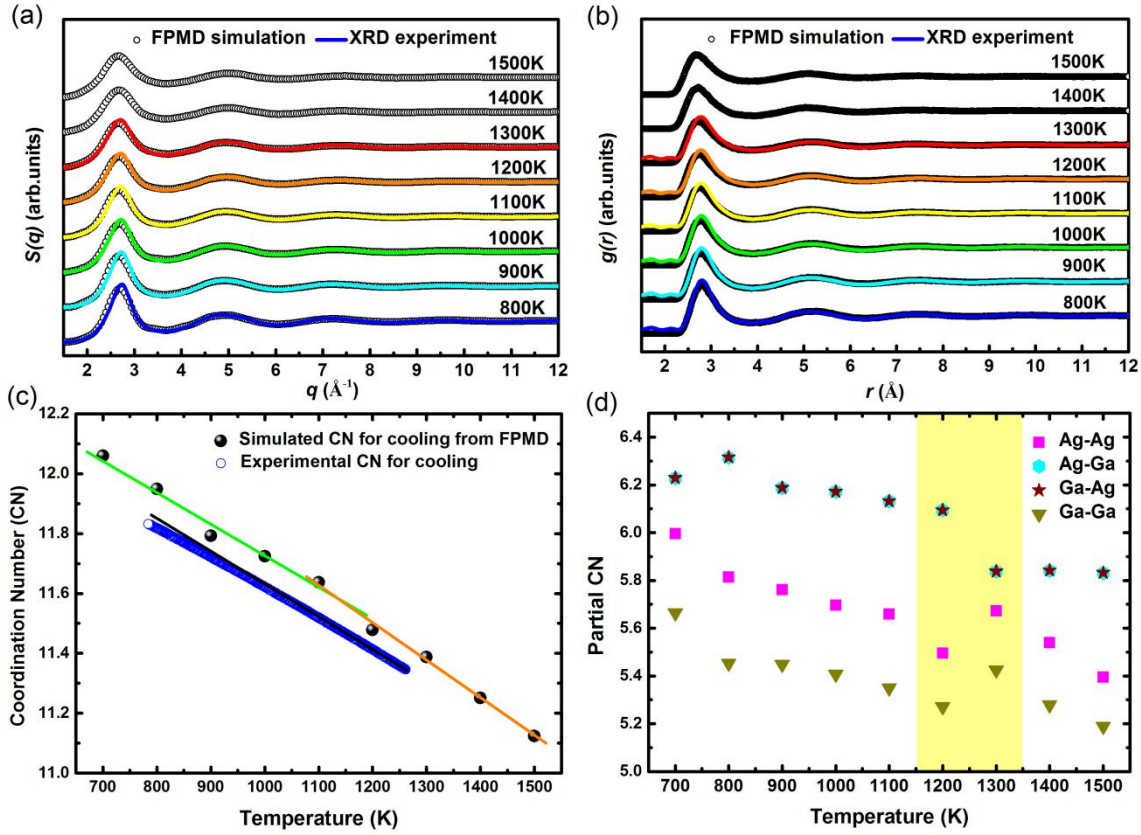

Fig. 3 Y. Su et al.,

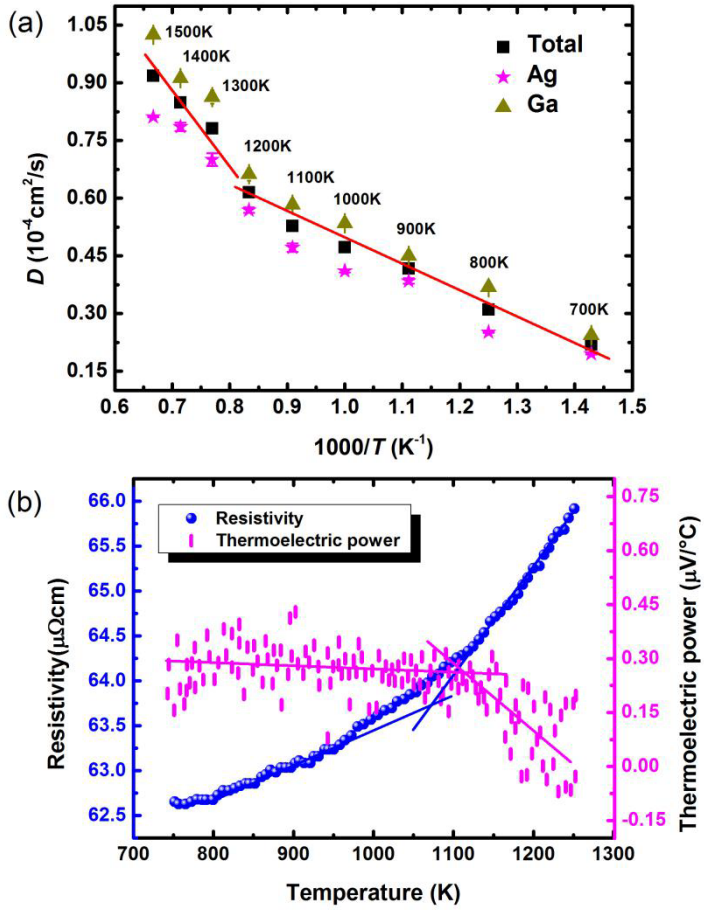

Fig. 4 Y. Su et al.,